HTD-Vol. 15

Thermal-Hydraulics in Nuclear Power Technology

presented at

20TH NATIONAL HEAT TRANSFER CONFERENCE
MILWAUKEE, WISCONSIN
AUGUST 2-5, 1981

sponsored by

THE HEAT TRANSFER DIVISION, ASME

edited by

K. H. SUN
ELECTRIC POWER RESEARCH INSTITUTE

S. C. YAO
CARNEGIE-MELLON UNIVERSITY

P. MARINKOVICH
WESTINGHOUSE ELECTRIC CORPORATION

V. K. DHIR
UNIVERSITY OF CALIFORNIA AT LOS ANGELES

THE AMERICAN SOCIETY OF MECHANICAL ENGINEERS
United Engineering Center 345 East 47th Street New York, N. Y. 10017

Library of Congress Catalog Card Number 81-65616

PREFACE

The public consciousness of the importance of the nuclear power as a viable energy option and its awareness of the potential safety issues have made nuclear power an area of enormous interest to the technical community. Thermal-hydraulics, i.e., the transport of energy and flow, is a major engineering discipline that deals with the performance of the nuclear power systems and the operation of nuclear plant components. This bound volume is a compilation of the papers presented at the ASME sessions on "Thermal-Hydraulics in Nuclear Power Technology" at the 20th National Heat Transfer Conference. The sessions are organized by the ASME K-13 Nucleonics Heat Transfer Committee of the Heat Transfer Division. This volume represents an advance of the state-of-art of the heat transfer field.

This volume covers the fundamental theories and phenomena, the performance characteristics of reactor components as well as the behavior of simulated nuclear systems and test reactors. In the fundamental area, the papers are associated with the heat transfer due to condensation in counter-current flooding, the hydrodynamics of a submerged vapor jet, the hydrodynamic criterion of flooding, the prediction of boiling transition, and the striping at the interface of thermal stratification. The papers that deal with the performance characteristic of reactor components include the study of the transient analysis of accumulators and the modes of natural circulation in U-tube steam generators for light water reactors and thermal fluctations in the steam generator of a fast breeder reactor. The papers in the category of plant system behavior are the study of the response of a scaled boiling water reactor system during a loss-of-coolant accident and the modeling of turbulent flow in the Fast Flux Test Facility.

It is hoped that this bound volume does not merely represent another addition to the rapid-growing literature, but to advance the understanding and the capability of modeling the nuclear power systems.

K. H. Sun
Electric Power Research Institute

S. C. Yao
Carnegie-Mellon University

CONTENTS

CONDENSATION HEAT TRANSFER AND FLOODING IN A COUNTER-CURRENT SUBCOOLED LIQUID AND SATURATED VAPOR FLOW

F. Dobran
Long Island City, New York

ABSTRACT

The paper develops an analysis of flooding with condensation heat transfer in a vertical tube. The two-phase flow pattern is assumed to be annular with the subcooled liquid adjacent to the tube surface. The core of the tube consists of a homogeneous mixture of saturated vapor and liquid droplets.

Examination of the void fraction envelope of the combined heat transfer and hydrodynamic equations revealed the existence of a flooding solution in which the parameters of its description are the ratio of gravity to viscous forces, buoyancy number, Bond number, liquid droplets entrainment parameter, subcooling number, Prandtl number, and the tube length parameter. Heat transfer results revealed that higher volumetric flooding fluxes are possible compared to the adiabatic flow. At higher subcooling numbers the results also showed a hysteresis effect which is more pronounced at lower Prandtl numbers and for shorter tubes.

The adiabatic flooding solution compared well with the experimental data of air-water and air-oil for smooth tube ends. For non-smooth tube ends, good comparison is achieved at higher liquid volumetric fluxes. The heat transfer flooding results compared satisfactorily with the experimental data of steam and water.

NOMENCLATURE

A	Flow cross-sectional area
Bo	Buoyancy number, $1-\rho_g/\rho_1$
Cp	Specific heat at constant pressure
D	Tube internal diameter
D^*	Tube diameter parameter, $D/\left(\frac{\sigma}{g(\rho_1-\rho_g)}\right)^{\frac{1}{2}}$, or Bond number
e	Entrainment parameter, $\lvert M_d/M_1 \rvert$
f	Friction coefficient
g	Gravitational constant
h	Local heat transfer coefficient
$\bar{h}$	Average heat transfer coefficient, $\int_0^L h\, dz/L$
h_{lg}	Enthalpy of evaporation
I_i	Constant in equation (15)
I_w	Constant in equation (13)
J	Volumetric flux, $M/(\rho A)$
J^*	Non-dimensional volumetric flux, defined by equation (17)
k	Thermal conductivity
L	Tube length
l	Perimeter for heat transfer, $\pi D/4$
M	Mass flow-rate
N_1	Ratio of gravity to viscous forces parameter, $(gD^3\rho_1(\rho_1-\rho_g)/\mu_1^2)^{\frac{1}{2}}$
Nu	Nusselt number, hz/k_1
p	Static pressure
Pr	Prandtl number
q	Heat flux
Re_1	Film Reynolds number, $M_1 D/(A\mu_1)$
S_{1i}	Subcooling number, $Cp_1(T_s-T_{1i})/h_{lg}$
St	Stanton number, $Nu/(Re_{1i}Pr_1)$
T_1	Liquid film bulk temperature
T_o	Reference temperature
W	Average fluid velocity
z	Axial distance along the tube, Figure 1

Greek Symbols

α	Void fraction, defined by equation (11)
η	Condensation efficiency, defined by equation (7')
μ	Absolute viscosity
ξ	Perimeter
ρ	Density
σ	Surface tension
τ	Shear stress

Subscripts

c	Pertains to the core
d	Pertains to the liquid droplets
g	Gas or vapor
i	Liquid film-vapor core interface
1	Pertains to the liquid film
$1i$	Pertains to the liquid film at the entrance to the tube
$1t$	Liquid film and liquid droplets
s	Saturation value

I. INTRODUCTION

Condensation of saturated or superheated vapor onto a counter-current flowing subcooled liquid has an application in the design of a pressurized water reactor (PWR) downcomer. When the loss-of-coolant accident (LOCA) occurs in the reactor, due to the break of a pipe in the primary coolant system, emergency core cooling (ECC) water is injected into the annular space which surrounds the reactor core in order to flood and cool the core. Some of the steam which is generated in the reactor core attempts to exit from the core through the annular space in a counter-current flow arrangement. The upflowing steam condenses onto the downflowing injected water, and if the steam flow-rate is sufficiently large, the steam flow limits the water supply rate to the reactor core. Under such a flooding situation, core cooling can be greatly hampered, and with further increase in the steam flow, the injected water is bypassed out from the broken leg. The design of PWR must prevent the occurrence of this situation with the proper design of an ECC system.

The understanding of fluid mechanics and heat transfer in a flooding situation is, therefore, of considerable interest, and their relative importance has not been fully investigated.

Previous Work

Flooding in the presence of heat transfer has been studied by Liu, Collier and Cudnik (1), Segev and Collier (2), and Liu and Collier (3) for the purpose of understanding the PWR downcomer thermal-hydraulics. These authors chose an annular flow configuration with liquid which flows adjacent to the downcomer walls and with saturated vapor which flows upwards through the annular core region. In Ref. 1 a heat transfer analysis is developed for the liquid film bulk temperature distribution as a function of the local liquid film mass flow-rate and the liquid film mass flow-rate at the inlet into the downcomer annulus. An expression was also developed for the local mass flow-rate of the condensed vapor in terms of the 'condensation efficiency' or the heat transfer coefficient. Flooding in the presence of heat transfer was accounted for by modifying the Wallis's (4) adiabatic flooding correlation for the local change in the vapor volumetric flux, i.e.

$$(J_g^* - \eta\lambda J_{1i}^*)^{\frac{1}{2}} + (\frac{\rho_g}{\rho_1})^{\frac{1}{4}} J_1^{*\frac{1}{2}} = \text{constant} . \qquad (1)$$

In the experiments of Liu et al. (1) no significant difference in flooding fluxes is found between the steam-water at low subcoolings and the air-water mixture in an adiabatic flow. In a later study, Segev and Collier (2) determined that the empirical coefficients which enter into the flooding model of equation (1) are test-geometry dependent, and at large subcoolings that the comparison between the analysis and the experiment is not as satisfactory as at low liquid subcoolings.

Recently, Liu and Collier (3) carried out an experimental study of the counter-current condensation of steam onto the subcooled water in an adiabatic tube and determined a correlation for the average heat transfer coefficient. They also observed a hysteresis effect in the flooding curves when the steam flow was increased from zero value to the point of complete liquid by-pass and when it was decreased to zero again. Tien (5) has alluded to the possibility of such a hysteresis effect in the heat transfer flooding curves by examining equation (1) for different values of the liquid subcoolings.

Counter-current condensation with flooding provides very interesting physics, and much of this physics is at the present incompletely understood. In part this is because of the complexity in carrying out accurate physical modeling of flooding phenomena and because of absence of the experimental data. In flooding without heat transfer in a tube, flooding is affected by the tube inlet configurations (Wallis (4), Tien et al. (6) and Bharathan et al. (7)), and on the methods by which the two-phases are introduced into the tube. With the addition of heat transfer, the local momentum balance in the flow field is continuously readjusted to account for the interphase momentum transfer which results from the condensing mass flux. In the heat transfer experiments carried out to date, no significant difference between heat transfer and adiabatic flooding curves is observed, and no analysis has been developed from fundamental principles in order to investigate the parameters which effect flooding in the presence of heat transfer.

Problem Under Investigation and Objectives of the Paper

The paper has the objective to extend the study of heat transfer and flooding hydrodynamics in a tube with an adiabatic wall in which saturated vapor is condensing onto a counter-current flowing subcooled liquid. The flow model is illustrated in Figure 1. The model consists of a time invariant liquid film thickness which is adjacent to the tube wall, and of a homogeneous mixture of liquid droplets which are entrained in the saturated vapor core. The positive flow direction is vertically downward and at the outset the following assumptions are made in the analysis:

1. The flow field can be described by two velocity fields, one for the liquid film and the other for the vapor core.
2. Viscous dissipation and kinetic energy effects are negligible.
3. Pressure is uniform across the tube cross-sectional area.
4. The vapor core enthalpy is primarily due to the saturated vapor.
5. There is no axial conduction in the liquid film.
6. The interface between the liquid film and the vapor core is, on the average, smooth.
7. Constitutive equations for the wall friction and liquid film-vapor core interface friction, which are described in Section II, adequately represent the phenomena under investigation.
8. Fluid properties are constant.
9. Liquid film inertia, and liquid film and vapor core velocities have flat profiles.
10. Axial shear stresses are negligible.

With the foregoing considerations, the flow field is modeled by the one-dimensional form of conservation equations for mass, momentum and energy which are described, as for example, by Dobran (8).

The specific objectives of the paper are the following:

1. To develop heat transfer expressions for arbitrary values of the liquid subcoolings.
2. To derive an adiabatic flooding model where the parameters of its description are the ratio of gravity to viscous forces, the Bond number, the buoyancy number, and the liquid droplets entrainment parameter.
3. To show how the entrainment parameter can be utilized to explain the trend in the experimental data.
4. To develop flooding curves with condensing heat transfer, and to show how the additional parameters in the form of subcooling number, Prandtl number and the tube length to the diameter ratio enter into their description.

II. ANALYSIS

Heat Transfer Analysis

Conservation of mass for the two-phase mixture requires that

$$\frac{d}{dz}(M_1 + M_c) = 0 , \qquad (2)$$

where M_1 is the liquid film mass flow-rate and M_c is the core mass flow-rate. The later is the sum of liquid droplets and vapor mass flow-rates, $M_c = M_d + M_g$.

Since the core flow is assumed saturated, only one energy equation is necessary to consider. For the two-phase mixture this equation is of the form

$$\frac{d}{dz}(M_1 Cp_1(T_1 - T_o) + M_c h_c) = q_w \xi_w = 0 . \qquad (3)$$

In the above expression, T_1 is the liquid film tempera-

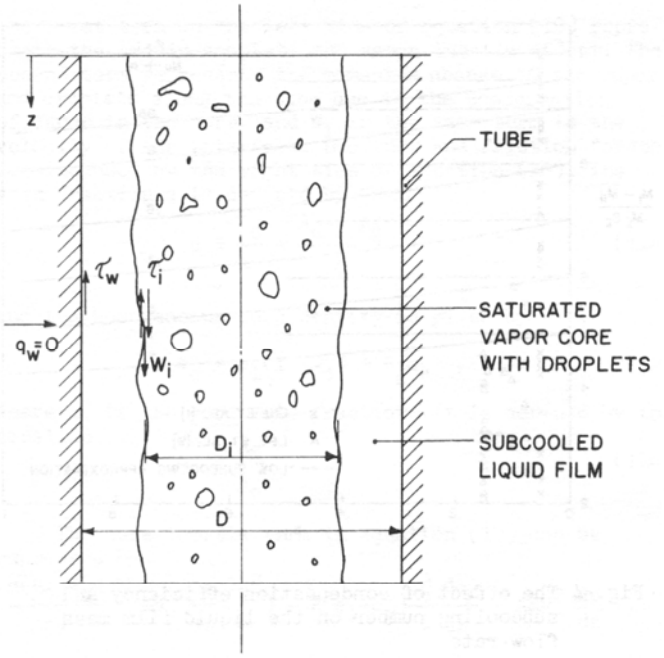

Fig. 1 Two-phase flow configuration in a tube

ture, T_c is the reference temperature, and h_c is the core enthalpy and by assumption it is equal to the saturated vapor value.

Integrating equation (3) from z=0 where $M_l = M_{li}$ and $T_l = T_{li}$ to z>0, and utilizing equation (2) to eliminate M_c, yields the liquid film bulk temperature distribution along the tube, i.e.

$$\frac{T_l - T_{li}}{T_s - T_{li}} = \left(1 - \frac{M_{li}}{M_l}\right) \frac{1 + S_{li}}{S_{li}} \quad , \qquad (4)$$

where T_s is the saturation temperature and S_{li} is the liquid subcooling number defined by

$$S_{li} \equiv \frac{Cp_l(T_s - T_{li})}{h_{lg}} \quad .$$

The local heat transfer coefficient, h, can be defined from the liquid film-vapor core interface energy balance

$$lh(T_s - T_l) \equiv h_{lg} \frac{dM_l}{dz} \quad . \qquad (5)$$

l is the heat transfer perimeter and in this paper it is chosen as the ratio of tube flow area to the tube diameter, $(\pi D/4)$. The average heat transfer coefficient, $\bar{h} \equiv (\int_0^L h\, dz)/L$, and the average Nusselt number, $\bar{Nu} \equiv \bar{h}z/k_l$, are obtained by integrating equation (5) and utilizing equation (4).

$$St \equiv \frac{\bar{Nu}}{Re_{li}Pr_l} = (1 + S_{li})\left[\ln\{1 + \frac{1}{(1+S_{li})} \frac{T_l - T_{li}}{T_s - T_l}\} - \frac{S_{li}}{(1+S_{li})\frac{T_s - T_l}{T_l - T_{li}}} \right] \qquad (6)$$

Re_l is the liquid-film Reynolds number which is defined by

$$Re_l \equiv \frac{M_l D}{A\mu_l} = \frac{DJ_l\rho_l}{\mu_l} \quad ,$$

and St is a form of the Stanton number.

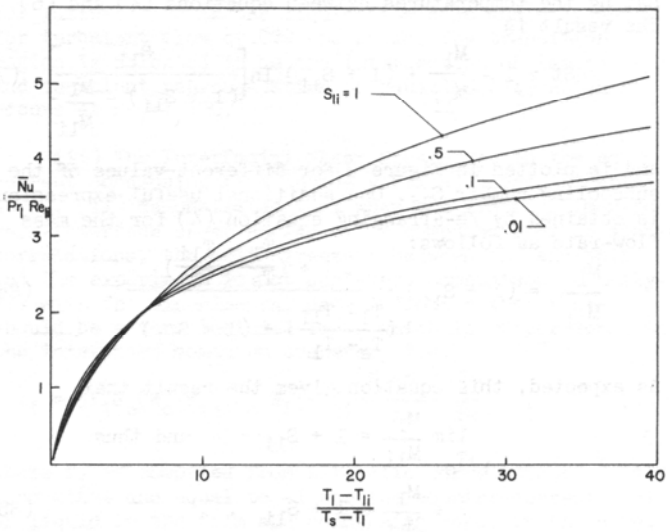

Fig.2 Relationship between the average Nusselt number and the liquid film bulk temperature for varying subcooling numbers

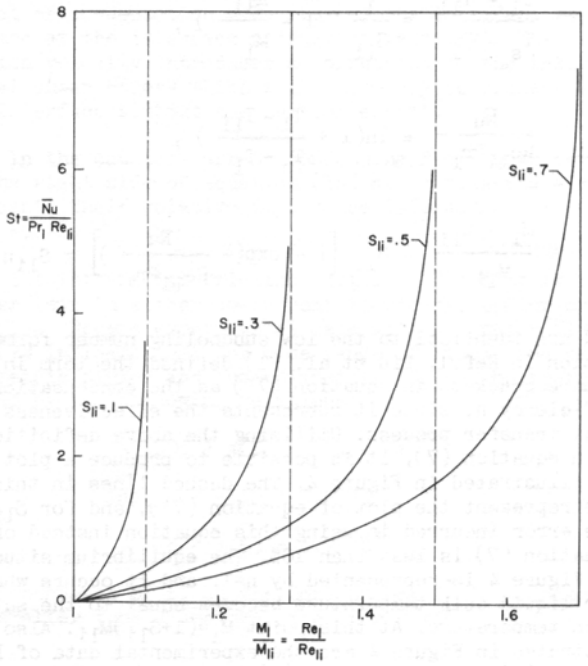

Fig.3 Relationship between the average Nusselt number and the film mass flow-rate for varying subcooling numbers

A plot of equation (6) is illustrated in Figure 2 with the subcooling number as the parameter. At large temperature ratios, $(T_l - T_{li})/(T_s - T_l)$, which occur far downstream from the top of the tube, there are considerable differences between average Nusselt numbers at higher and lower subcooling numbers. The low subcooling number formulation of Ref. 1, therefore, underpredicts the heat transfer rate if it is applied to subcooling numbers of greater than about .1 in long tubes.

An expression which is useful for determining the average Nusselt number from the experimental measurement of the local film mass flow-rate is obtained by elimi-

nating the temperatures between equations (4) and (6). The result is

$$St = 1 - \frac{M_l}{M_{li}} + (1 + S_{li}) \ln\left[\frac{S_{li}}{(1 + S_{li}) - \frac{M_l}{M_{li}}}\right], \quad (7)$$

and is plotted in Figure 3 for different values of the subcooling number S_{li}. One additional useful expression is obtained by re-arranging equation (4) for the mass flow-rate as follows:

$$\frac{M_l}{M_{li}} = (1 + S_{li}) \frac{1 + \left(\frac{T_l - T_{li}}{T_s - T_l}\right)}{\left(\frac{T_l - T_{li}}{T_s - T_l}\right) + (1 + S_{li})} . \quad (8a)$$

As expected, this equation gives the result that

$$\lim_{T_l \to T_s} \frac{M_l}{M_{li}} = 1 + S_{li} \qquad \text{and thus}$$

$$1 \leq \frac{M_l}{M_{li}} \leq 1 + S_{li} . \quad (8b)$$

For subcooling numbers which are much less than one, equations (4), (6) and (7) are reduced respectively to

$$\frac{T_l - T_{li}}{T_s - T_l} \simeq \frac{1}{S_{li}} \left(1 - \frac{M_{li}}{M_l}\right), \quad (4')$$

$$\frac{\bar{N}u}{Re_{li} Pr_l} \simeq \ln\left(1 + \frac{T_l - T_{li}}{T_s - T_l}\right), \quad (6')$$

$$\frac{M_l - M_{li}}{M_{li}} \simeq S_{li}\left[1 - \exp\left(-\frac{\bar{N}u}{Re_{li} Pr_l}\right)\right] \equiv S_{li}\eta \quad (7')$$

and are identical to the low subcooling number formulation in Ref.1. Liu et al. (1) defined the term in square brackets in equation (7') as the condensation efficiency η, since it represents the effectiveness of heat transfer process. Utilizing the above definition of η in equation (7), it is possible to produce a plot which is illustrated in Figure 4. The dashed lines in this figure represent the plot of equation (7'), and for $S_{li}<.5$ the error incurred in using this equation instead of equation (7) is less than 10%. The equilibrium situation in Figure 4 is represented by $\eta=1$, and it occurs when the liquid bulk temperature becomes equal to the saturation temperature. At this point $M_l=(1+S_{li})M_{li}$. Also illustrated in Figure 4 are the experimental data of Liu et al. (1), and Lee et al. (9) from the co-current condensation study in a horizontal duct. These data indicate that in most cases full equilibrium flow is not achieved.

The heat transfer analysis presented above is equally valid for co-current and counter-current condensation of saturated vapor onto a subcooled liquid in adiabatic ducts of arbitrary cross-section. As such, the analysis can form the basis for data reduction for arbitrary values of the subcooling number and bring consistency to the large class of problems. The inconsistency in the literature with respect to the above remark is evident in References 3 and 9 where the average Nusselt number is computed from the experimentally measured values of the liquid mass flow-rates in completely different ways. The outcome of this inconsistency is reflected in heat transfer correlations which are presented in the literature.

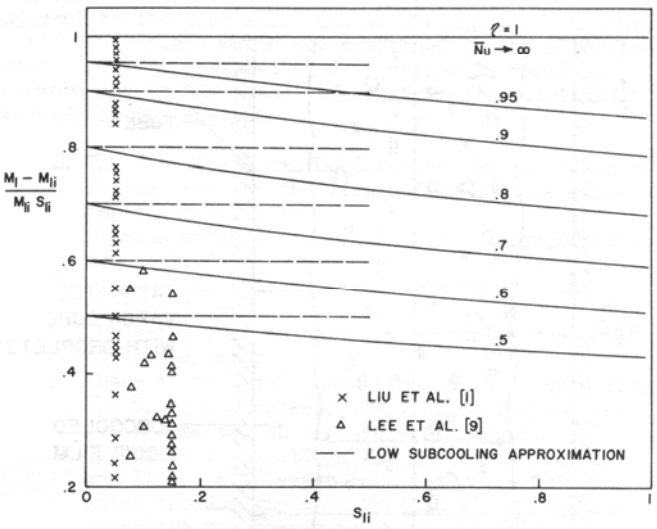

Fig. 4 The effect of condensation efficiency and subcooling number on the liquid film mass flow-rate

The heat transfer analysis is complete when the variation of liquid mass flow-rate is expressed in terms of the axial distance along the tube. Liu and Collier (3) carried out extensive low-subcooling number measurements in counter-current condensing flows with steam and water in a tube and determined that the average Nusselt number can be represented by the following expression:

$$\bar{N}u = .00428\left(\frac{z}{D}\right)^{.14} J_l^{*.81} N_l^{1.477} . \quad (9)$$

The range of validity of equation (9) is as follows:

$$S_{li} \; ; \; .07 - .14$$

$$N_l J_l^* = 4M_l/\mu_l \; ; \; 10 - 10^4$$

$$z/D \; ; \; .7 - 30$$

$$J_{li}^* \; ; \; .05 - .16 .$$

The non-dimensional group N_l (Wallis (4)) represents the ratio of gravity to viscous forces and appears more visibly in the hydrodynamic analysis of the next section. J_l^* is the non-dimensional liquid film volumetric flux and is defined by equation (17).

The combination of equations (7) and (9) yields an expression in which z/D is related to the liquid film mass flow-rate and to the independent parameters of the problem (N_l, S_{li}, Pr_l, and Re_{li} or J_{li}^*). These equations will be used in the next section.

Hydrodynamic Analysis

Momentum equations can be written for the two-phase mixture, for the liquid film, and for the liquid droplets and vapor core. Since the formulation is carried out in terms of two velocity fields, only two of these equations need to be considered. By eliminating the pressure gradient between the momentum equation for the two-phase mixture and a momentum equation for the liquid film, the following equation is obtained:

$$(\alpha-1)\frac{d}{dz}(M_c W_c) + W_i \frac{dM_c}{dz} = \alpha(1-\alpha)gA(\rho_l - \rho_c) - \alpha\tau_w \xi_w + \tau_i \xi_i . \quad (10)$$

The first term on the left side of equation (10) represents the liquid-droplets and vapor inertia effect. The second term represents the momentum change of the vapor and droplets along the tube due to the condensation of vapor in the core, and W_i in the same term is the velocity of the interface. Buoyancy and friction forces are included on the right side of equation (10). The void fraction α is defined by

$$\alpha \equiv \frac{A_c}{A} = \frac{A_d + A_g}{A} \quad , \tag{11a}$$

and the homogeneous core density is given by

$$\rho_c = \rho_l(1 - \alpha_c) + \rho_g \alpha_c \quad , \tag{12}$$

where α_c is the core void fraction. It is defined by the equation

$$\alpha_c \equiv \frac{A_g}{A_c} \quad . \tag{11b}$$

The core inertia term in equation (10) can be expressed by

$$\frac{d(M_c\, W_c)}{dz} = A\rho_c \frac{d}{dz}\left(\frac{J_c^2}{\alpha}\right) - A(\rho_l - \rho_g)\frac{J_c^2}{\alpha}\frac{d\alpha_c}{dz} + A\alpha M_\infty^2 \frac{dp}{dz} \quad ,$$

where J_c is the core volumetric flux and is related to M_c by:

$$M_c = \rho_c A J_c = \rho_c A(\alpha) W_c \quad .$$

M_∞ is the two-phase Mach number and is given by

$$M_\infty^2 = \frac{M_c^2}{A^2\alpha^2\rho_c^2}\frac{d\rho_c}{dp} \quad .$$

Of the three terms on the right of the above equation, the first term is most significant. Its inclusion into the theory presented below is not simple and has been, therefore, neglected. In the case of large subcoolings this neglect might not turn out to be justifiable. The effect of variation of the core void fraction along the tube due to the liquid-droplets-entrainment and the effect of the compressibility of the vapor is expected to be of the second order in importance when compared to buoyancy and viscous forces, and were neglected in the analysis.

The expressions for interface velocity, wall shear stress and interfacial shear stress were chosen as follows:

i) Interface Velocity, W_i.

$$W_i = I_w W_l \quad . \tag{13}$$

In the adiabatic co-current annular flow, plausible range of I_w is 1.5 to 3, and is assumed to be valid in the present analysis (Wallis (10)).

ii) The Wall Shear Stress, τ_w. The wall shear stress is expressed by the usual relation

$$\tau_w \equiv f_w \tfrac{1}{2}\rho_l W_l |W_l| = f_w \tfrac{1}{2}\rho_l \frac{J_l|J_l|}{(1-\alpha)^2} \quad , \tag{14}$$

and neglecting the film thickness effect on the distribution of f_w (Wallis (10)), the wall friction factor is represented by the equation

$$f_w = \frac{c}{|Re_l|^n} \quad .$$

For laminar flow in the liquid film c=16 and n=1, and for turbulent flow c=.079 and n=.25. The transition region is selected to be the intersection of laminar and turbulent representation of equation (14) which occurs at Re_l=1,190.

iii) The Interfacial Shear Stress, τ_i. In the co-current condensing flow inside vertical tubes, Linehan et al. (11) demonstrated that when the liquid film-vapor core interface shear stress τ_i is computed from adiabatic correlations, the best agreement between the analysis and the experiment is not achieved. Comparison of analysis with the experimental data indicates that there should be a term included in τ_i which is proportional to the interphase momentum transfer, i.e.

$$\tau_i = \tfrac{1}{2} f_i \rho_c (W_c - W_i)|W_c - W_i| + I_i \frac{(W_c - W_i)}{\xi_i}\frac{dM_l}{dz} \quad , \tag{15}$$

where f_i is computed from adiabatic correlations. I_i is a constant and equal to -1 for the counter-current flow of liquid in the film and condensing vapor in the core.

The form of equation (15) is plausible also if a Couette turbulent layer with suction (Kays and Crawford (12)) is considered in the region of vapor core in the vicinity of the liquid film-vapor core interface. The effect of condensation mass flux at the interface is to produce at the interface a 'suction velocity'. The suction velocity introduces a correction to the interfacial shear stress which would normally be present at the interface without the suction effect.

In the counter-current condensing flow, both terms on the right side of equation (15) are considered significant. Their relative importance is discussed in the next section.

The interfacial friction factor in flooding is larger than in either co-current liquid-gas upflow or downflow. Recent experimental data with air-water flooding (7) indicate that for wide range of liquid and gas volumetric fluxes and tube diameters, f_i can be represented by the following relations:

$$f_i = .005 + a(D^*/2)^b(1 - \sqrt{\alpha})^b \tag{16}$$

$$\log_{10} a = -.56 + 9.07/D^*$$

$$b = 1.63 + 4.74/D^* \quad .$$

The dependence of f_i on the Bond number D^* is pronounced for smaller tube diameters, i.e. for $D^* < 50$.

To complete the analytic description of the problem under investigation, it is useful to non-dimensionalize equation (10). Towards this end the core volumetric flux is defined by $J_c = \alpha W_c$, liquid film volumetric flux by $J_l = (1-\alpha)W_l$, and vapor volumetric flux by $J_g = \alpha\alpha_c W_c = \alpha_c J_c$. The volumetric fluxes are non-dimensionalized according to the expressions

$$J_g^* = J_g\left(\frac{\rho_g}{gD(\rho_l - \rho_g)}\right)^{\frac{1}{2}} \quad , \quad J_l^* = J_l\left(\frac{\rho_l}{gD(\rho_l - \rho_g)}\right)^{\frac{1}{2}} \quad , \tag{17}$$

and the non-dimensional axial coordinate in the tube is defined by $z^* = z/D$. Utilizing above definitions and equations (11) to (16), equation (10) becomes

$$F \equiv \psi^2(1-\alpha)^2 J_g^*|J_g^*| - \frac{\alpha^{\frac{3}{2}}}{2f_i}(1-\alpha)\frac{dJ_g^*}{dz^*}\left[I_i\psi\left(\frac{1-\alpha}{\alpha}\right)J_g^* + I_w\left(\frac{\rho_g}{\rho_1}\right)^{\frac{1}{2}}\alpha_c J_1^*\right] - \frac{\alpha^{3/2}}{f_i}\alpha\left(\frac{\rho_g}{\rho_c}\right)\left[\frac{2c}{N_1^n}\alpha_c^2 J_1^*|J_1^*|^{1-n} - \alpha_c^3(1-\alpha)^3\right] = 0 \quad . \qquad (18)$$

In the above equation

$$\psi \equiv 1 - \frac{W_i}{W_c} = 1 - I_w\frac{\alpha\alpha_c}{1-\alpha}\left(\frac{\rho_g}{\rho_1}\right)^{\frac{1}{2}}\frac{J_1^*}{J_g^*} \quad ,$$

and the parameter

$$N_1 \equiv \left(\frac{gD^3\rho_1(\rho_1-\rho_g)}{\mu_1^2}\right)^{\frac{1}{2}}$$

represents the ratio of gravity to viscous forces. The transition point between laminar and turbulent flow in the liquid film is now expressed by $J_1^* = 1{,}190/N_1$.

The number N_1 is similar in appearance to the Grashof number (Gr) in natural convection flows. I do not, however, prefer to call N_1 the Grashof number since it is not a consequence of the buoyancy forces which are induced by the temperature gradient as in the case of Gr. Perhaps N_1 should be called the two-phase Grashof number. In this paper I will continue to call N_1 the ratio of gravity to viscous forces parameter.

The core void fraction, α_c, is very close to one in most applications. Nevertheless, the density ratio ρ_g/ρ_c in equation (18) is very sensitive to its value. In the analysis herein α_c is related to the entrainment parameter e which is defined as follows:

$$e = \left|\frac{\text{mass flow-rate of liquid droplets in the core}}{\text{mass flow-rate of the liquid film}}\right|$$

Hence it readily follows that

$$\alpha_c = \frac{1}{1 + e\left(\frac{\rho_g}{\rho_1}\right)^{\frac{1}{2}}\left|\frac{J_1^*}{J_g^*}\right|} \quad . \qquad (19)$$

In general, the entrainment varies along the tube and can be correlated by the interfacial shear stress and by the liquid film thickness (Ref. 13). The present analysis, however, assumes that the entrainment e is an independent parameter. As will be seen below in the results, this simple assumption is adequate.

The effect of condensing heat transfer in equation (18) is expressed by the term dJ_g^*/dz^*. It is obtained from equations (4) and (5) by utilizing the above non-dimensionalization procedure The result is:

$$\frac{dJ_g^*}{dz^*} = \left[1-(1+S_{1i})\frac{J_{1i}^*}{J_1^*}\right]\frac{Nu\frac{D}{z}\alpha_c}{Pr_1 N_1}\left(\frac{\rho_g}{\rho_c}\right)\left(\frac{\rho_1}{\rho_g}\right)^{\frac{1}{2}} \quad . \qquad (20)$$

$Nu=hz/k_1$ is the local Nusselt number and in this paper it is obtained from equation (9) by differentiation, i.e.

$$Nu\frac{D}{z} = .14\bar{Nu}\left(\frac{.00428N_1^{1.477}J_1^{*.81}}{\bar{Nu}}\right)^{1/.14} + .81\frac{\bar{Nu}}{J_1^*}\frac{dJ_1^*}{dz^*} \quad . \qquad (21a)$$

The average Nusselt number is expressed by equation (7), and in the new nomenclature it is of the following form:

$$\bar{Nu} = N_1 Pr_1 J_{1i}^*\left\{1 - \frac{J_1^*}{J_{1i}^*} + (1+S_{1i})\ln\left[\frac{S_{1i}}{(1+S_{1i}) - \frac{J_1^*}{J_{1i}^*}}\right]\right\} \quad . \qquad (21b)$$

In equation (21a), dJ_1^*/dz^* is expressed in terms of dJ_g^*/dz^* if the continuity equation (2) is used. Hence

$$\frac{dJ_1^*}{dz^*} = -\left(\frac{\rho_c}{\rho_g}\right)\frac{1}{\alpha_c}\left(\frac{\rho_g}{\rho_1}\right)^{\frac{1}{2}}\frac{dJ_g^*}{dz^*} \quad . \qquad (21c)$$

Equations (9) and (18) to (21a,b,c) are sufficient to investigate flooding in a tube in the presence of condensing heat transfer. The arbitrary parameters of the problem are the following:

1. Ratio of gravity to viscous forces, N_1.
2. Density ratio (Buoyancy number), $Bo=1-\rho_g/\rho_1$.
3. Bond number, D^*.
4. Subcooling number, S_{1i}.
5. Prandtl number, Pr_1.
6. Entrainment parameter, e.
7. Dimensionless liquid volumetric flux at the tube inlet, J_{1i}^*.

Solution Procedure for Equation (18)

The flooding solution of equation (18) for the liquid and vapor volumetric fluxes was obtained by investigating the singularity set with respect to the void fraction α, or by setting

$$\frac{dF}{d\alpha} = G = 0 \quad , \qquad (22)$$

and eliminating α between these two equations. Examination of equations (18) and (22) revealed that a flooding solution exists for the downflowing liquid, $J_1^*>0$, and for the upflowing vapor, $J_g^*<0$. Since the equations are non-linear in J_1^* and J_g^*, their simultaneous solution has been carried out numerically with the two dimensional Newton-Raphson iteration scheme. This scheme is of the form

$$\begin{pmatrix} \left.\frac{\partial F}{\partial J_1^*}\right|^k & \left.\frac{\partial F}{\partial J_g^*}\right|^k \\ \left.\frac{\partial G}{\partial J_1^*}\right|^k & \left.\frac{\partial G}{\partial J_g^*}\right|^k \end{pmatrix}\begin{pmatrix} J_1^{*k+1} - J_1^{*k} \\ J_g^{*k+1} - J_g^{*k} \end{pmatrix} + \begin{pmatrix} F^k \\ G^k \end{pmatrix} = 0 \quad , \qquad (23)$$

where k denotes the iteration number. In all results presented in the paper, the computed values of the liquid and vapor volumetric fluxes were considered correct when the error between two successive iterations was less than 10^{-6}. On the average, 15 iterations produced the desired error tolerance.

III. RESULTS AND DISCUSSION

Before accepting the heat transfer flooding results it is necessary to test the theory against the experimental data for flooding in a tube in adiabatic flow.

Adiabatic Flooding Solution

In adiabatic flow $dJ_g^*/dz^*=0$ in equation (18) and flooding is described by the following equations:

$$-J_g^*|J_g^*| = \frac{3\alpha^{7/2}(1-\alpha)\alpha_c^3}{\psi^2\frac{\rho_c}{\rho_g}\left\{4\alpha f_i + (1-\alpha)\left[5f_i - 2\alpha\frac{df_i}{d\alpha}\right]\right\}} \qquad (24)$$

$$J_1^*|J_1^*|^{1-n} = \frac{N_1^n}{2c}\alpha_c(1-\alpha)^3\left[1 - \frac{6\alpha f_i}{4\alpha f_i + (1-\alpha)\left[5f_i - 2\alpha\frac{df_i}{d\alpha}\right]}\right] \qquad (25)$$

Equations (24) and (25) assume that the variation of ψ with α is negligible as is indeed the case. Inspection of these equations indicates that the flooding solution exists for $J_l^*>0$ and $J_g^*<0$.

The adiabatic flooding solution for $N_l=12,000$, $D^*=9.3$ and Bo=.9988 is shown in Figure 5 in the plot of $\sqrt{-J_g^*}$ versus $\sqrt{J_{lt}^*}$. The values of these parameters correspond to the air-water at atmospheric pressure and in .0254m diameter tube. The liquid volumetric flux represented in Figure 5 is the value composed of the liquid fluxes in the film and in the core, since it is this total value which is reported in experiments on flooding. The total liquid volumetric flux is related to the liquid film volumetric flux by $J_{lt}^*=(1+e)J_l^*$.

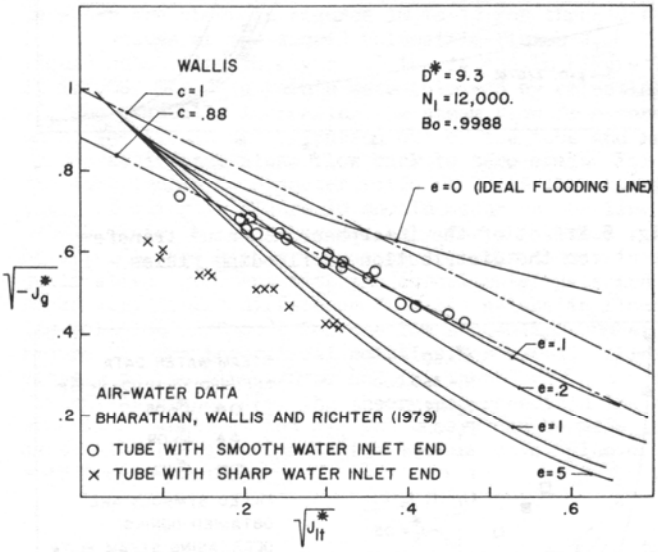

Fig. 5 Comparison of air-water experimental data with theory

The ideal flooding line in Figure 5 corresponds to the zero value of the entrainment parameter, and is seen to be only in qualitative agreement with the experimental data of Wallis (4) and Bharathan et al. (7). For non-zero value of the entrainment parameter, the analysis captures the experimental data very well except for tubes with sharp water inlet ends at low liquid volumetric fluxes. The entrainment of liquid in the gas or vapor core is caused by the breakdown of waves on the liquid-gas interface and at the tube ends when these ends are poorly streamlined. For air-water flooding data with smooth tube ends, the analysis agrees with the experiment if the value for an entrainment parameter is chosen to be .1. This value is reasonable, and future experimental studies should attempt the measurement of e. Flooding in tubes with non-smooth ends is represented in the analysis with higher values of the entrainment parameter than for tubes with smooth ends. At low liquid volumetric fluxes the theory overpredicts the experiment in Figure 5 for non-smooth tube ends. The disagreement can be attributed to the breakdown of liquid film flow or to the flow pattern which is not annular. More viscous liquids would tend to minimize this breakdown and the air-oil data in Figure 6 atest to this fact. At low liquid volumetric fluxes it is also possible to achieve a better comparison between the theory and the experiment by accounting for the variation of ψ with α in the analysis. This correction is, however, of the second order except at very high pressures.

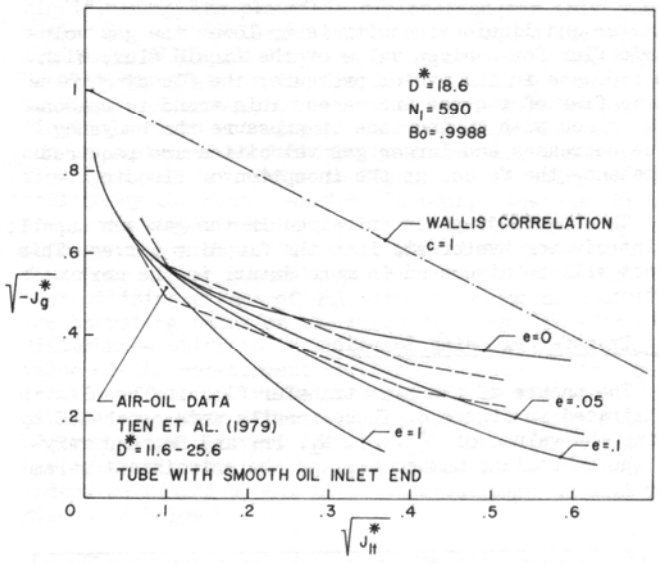

Fig. 6 Comparison of air-oil experimental data with theory

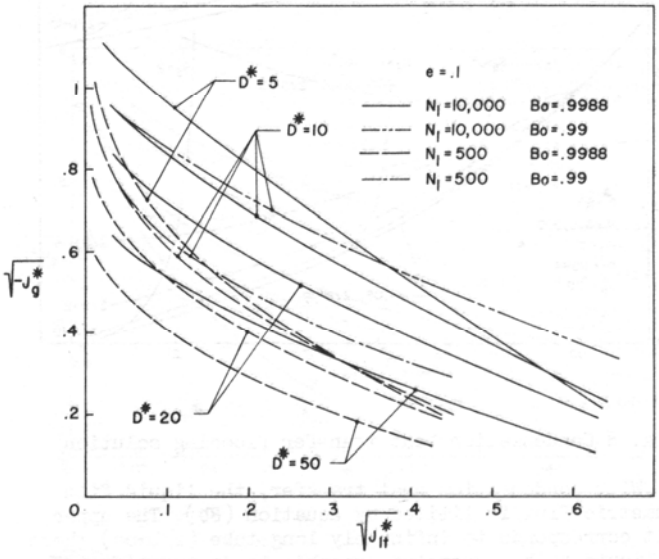

Fig. 7 The effect of liquid viscosity, system pressure and tube diameter on the distribution of adiabatic flooding fluxes

For large values of the entrainment parameter, the homogeneous flow of liquid droplets and gas will not occur. At low gas volumetric fluxes it is reasonable to set this limit to be at e=.1.

Comparison of the experimental data of Tien et al. (6) for air-oil flooding with theory is illustrated in Figure 6. The data envelope is well represented by an entrainment parameter which is equal to .05. Lower values for e are expected for viscous fluids.

The results from adiabatic analysis are summarized in Figure 7 for the entrainment parameter equal to .1. As shown in the figure, the effect of increasing tube

diameter and liquid viscosity is to lower the gas volumetric flux for a given value of the liquid flux. With the increase in the system pressure, the flooding volumetric flux of the gas increases. This trend is reasonable, since with an increase of pressure the buoyancy force decreases and larger gas velocities are required to balance the forces at the inception of flooding.

The liquid droplets entrained in the gas are capable of introducing hysteresis into the flooding curves. This effect will be discussed in more detail in the next section.

Heat Transfer Flooding Solution

The nature of the heat transfer flooding results is illustrated in Figure 8. These results were generated by fixing the values of J^*_{1i}, D^*, N_1, Pr_1 and Bo, and varying the subcooling number S_{1i} and the entrainment parameter e.

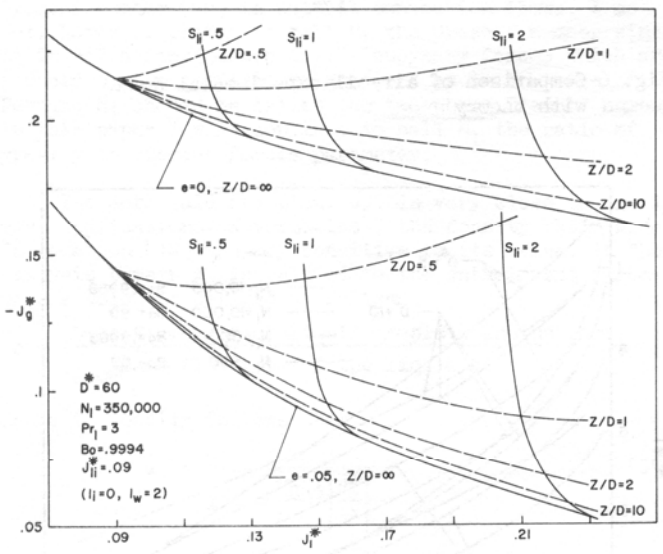

Fig. 8 Condensation heat transfer flooding solution

With condensation heat transfer, the liquid film volumetric flux is limited by equation (8b). The upper limit corresponds to infinitely long tube ($z/D \to \infty$) where the liquid bulk temperature reaches the saturation temperature. At this point the flow becomes adiabatic and the adiabatic flooding solution should apply. The results in Figure 8 are in agreement with this conclusion. Furthermore, flooding with heat transfer occurs at the bottom of the tube where the liquid and vapor volumetric fluxes have largest values. With tubes of finite length, the effect of condensation is to raise the flooding curve above the one in adiabatic flow, and this effect is more pronounced at higher subcooling numbers. The condensing heat and mass flux has the effect of bringing stability to flooding in a similar manner that suction brings stability to the boundary layers. On the contrary, the entrained liquid droplets destabilize the flooding curve as in the adiabatic flow situation. The liquid droplets in the vapor core preserve the shape of the heat transfer flooding curve and bring more closely together this curve and the adiabatic flooding curve. This behavior is reasonable, since the liquid droplets do not contribute in latent heat towards the condensing heat transfer rate.

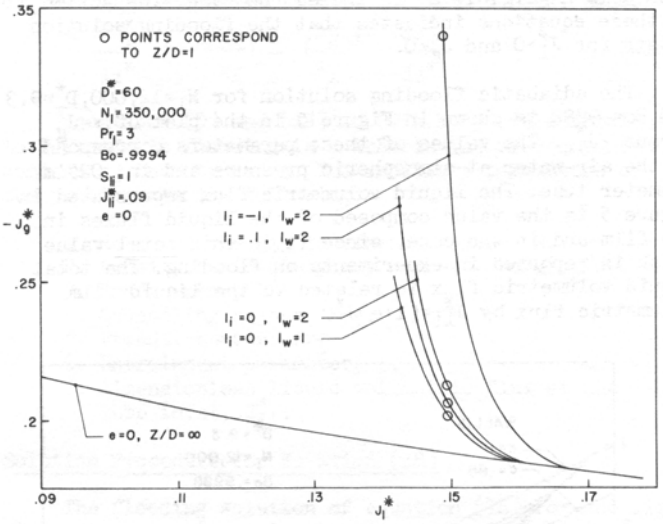

Fig. 9 Effect of the interphase momentum transfer on the distribution of flooding fluxes

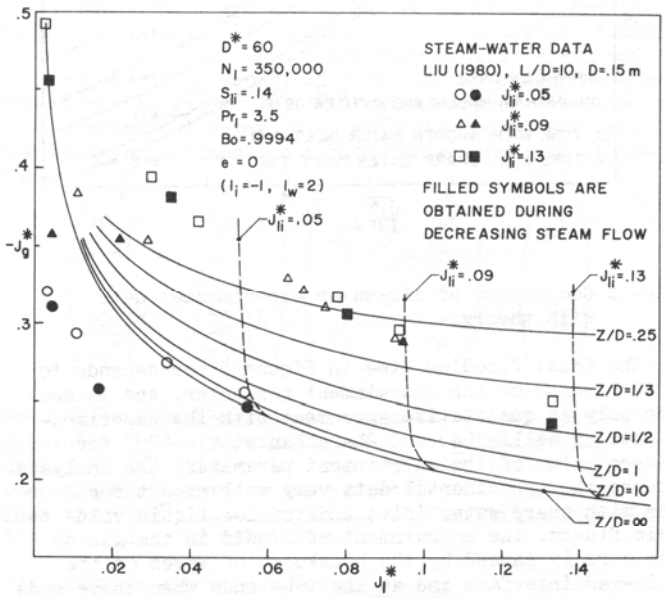

Fig. 10 Heat transfer flooding solution for liquid subcooling of .14 and comparison with the experimental data of steam and water

Figure 8 was generated by neglecting the effect of mass transfer on the interfacial shear stress in equation (15), and by setting the ratio of liquid-vapor interface velocity to the average liquid film velocity at 2. In Figure 9 these effects are investigated through the constants I_i and I_w. As this figure shows, the effect of changing the velocity ratio (I_w) by a factor of 2 does not change results significantly. The effect of condensing mass flux on the interfacial shear stress (parameter I_i) is, however, very important. Its negative value implies that in counter-current condensing flows the liquid-vapor interface friction is lower than in

adiabatic flow. The experimental data presented below attest to this fact.

Heat transfer flooding curves for fixed D^*, N_l, S_{li}, Pr_l, Bo and e=0 are illustrated in Figure 10 for different values of the tube length parameter z/D. These results were generated by connecting points of equal values of z/D when J^*_{li} is varied and with all other parameters remaining fixed. The presentation of results in the form of Figure 10 is important since it clearly shows the effect of tube geometry, and allows ready comparison of theory with the experimental data. For a given tube length and diameter, flooding states are represented on the line of constant z/D.

The experimental data of Liu and Collier (3), and Liu (14) for the counter-current condensation of steam on water are shown in Figures 10 to 12 for three different values of the liquid volumetric fluxes J^*_{li}. The liquid subcooling in Figure 10 is .14 and in Figure 11 it is .08. The data points were obtained by selecting J^*_{li} and gradually increasing the steam flow from zero until the liquid was by-passed out of the tube and then by decreasing the steam flow back to zero again. For the tube length to diameter ratio of 10 in the experiment, flooding in Figure 10 should occur on the line z/D=10. This, however, occurs only for the lowest value of J^*_{li}=.05. For higher values of J^*_{li}, the theory is in qualitative agreement with the experimental data and shows very little difference from the adiabatic flooding solution (z/D=∞). For the low subcooling number in Figure 11, the theoretical solution for z/D=10 falls very closely to the line z/D=∞ and is, therefore, not illustrated. At higher J^*_{li}, the theory underpredicts the experiment while at low J^*_{li} the theory can be made to agree with the experiment with the non-zero value of the entrainment parameter.

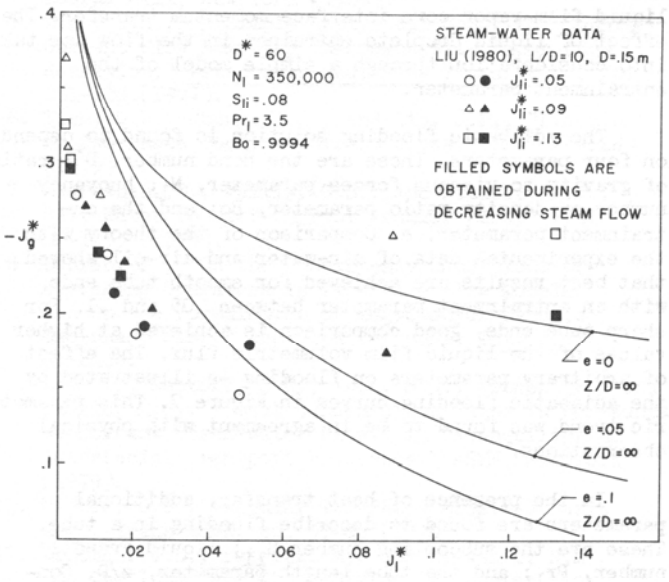

Fig. 11 Comparison of the experimental data at low liquid subcooling with the adiabatic flooding solution

The experimental data in Figure 10, for the subcooling number of .14 show no hysteresis effect during the decrease of steam flow from the liquid by-passed point, and the entrainment effect does not appear to be of significance. The plausible explanation for this observation is that at larger subcooling numbers the entrainment of liquid droplets is supressed by the high droplet deposition rate. The low subcooling number data in Figure 11 shows, however, that heat transfer and liquid droplets entrainment can cause hysteresis, and can be explained as follows: On increasing the steam flow from the zero value in Figure 11, flooding is controlled by the heat transfer. Flooding, however, brings about the liquid droplets entrainment which can be supressed only at sufficiently high interphase mass fluxes or higher subcoolings. At lower subcoolings, the destabilizing effect of entrainment predominates, and the operating point on the flooding curve can with slight disturbance shift to the flooding curve with the non-zero value of the entrainment parameter. In Ref. 3 the hysteresis effect in the data is associated with the subcooling number effect and not with the explanation offered above. At very high liquid subcoolings, the hysteresis in the heat transfer flooding curves can indeed be caused by S_{li} without entrainment as will be discussed below.

The experimental data for .05m tube diameter in Figure 12 at high and low liquid subcoolings show similar trend to the data in Figures 10 and 11. The effect of condensing heat flux in the data of Figure 12 at low D^* is more pronounced than in Figures 10 and 11 at high D^*. The theory is also qualitatively in accord with the experimental observation.

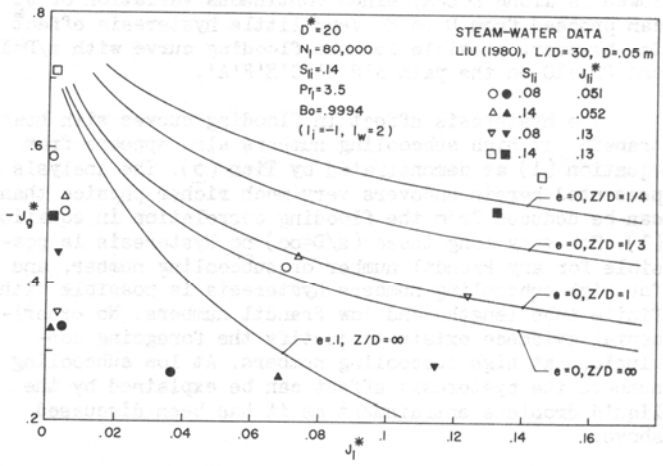

Fig. 12 Comparison of small tube diameter experimental data with theory

The effects of Prandtl number and tube length to diameter ratio on the flooding volumetric fluxes are illustrated in Figure 13 for the high subcooling number. Although the heat transfer correlation utilized in the model is outside the range of validity for this subcooling number, the qualitative solution behavior in Figure 13 should nevertheless be correct. The results illustrate that at higher subcoolings the Prandtl number can significantly affect the heat transfer flooding curve at high liquid volumetric fluxes. Lower Prandtl number fluids stabilize the flooding curve and can introduce hysteresis effect. The hysteresis effect in Figure 13 appears when the liquid volumetric flux is held fixed and the controlling variable is the vapor flux J^*_g. Thus starting with J^*_l at point A and tube geometry z/D=1, and increasing $-J^*_g$ to the point B on the curve with Pr_l=3, no change of the liquid flow occurs. At point B, however,

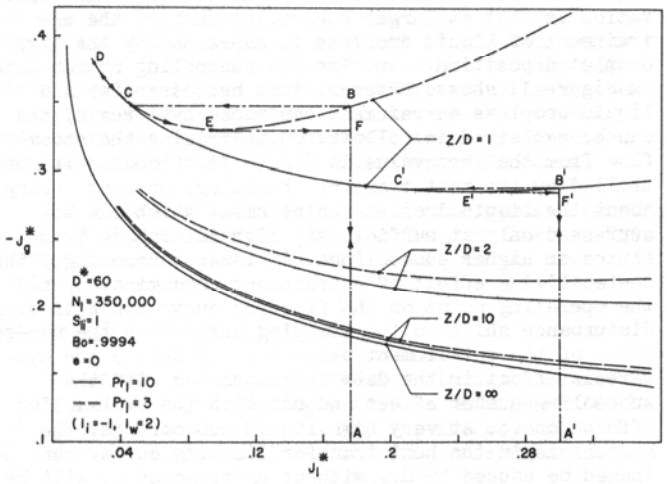

Fig. 13 The effect of Prandtl number and tube length on the distribution of flooding fluxes

a slight change in J_g^* shifts the operating point to the state at point C with considerably lower value of J_l^*. From point C to point D and from D to C, continuous changes in volumetric fluxes J_l^* and J_g^* are again possible. Upon decreasing $-J_g^*$ from D to A, the path followed is along DCEFA, since continuous variation of J_g^* can proceed from D to E. Very little hysteresis effect is, however, possible for the flooding curve with z/D=1 and Pr_l=10 on the path A'B'C'DC'E'F'A'.

The hysteresis effect in flooding curves with heat transfer at high subcooling numbers also appears from equation (1) as demonstrated by Tien (5). The analysis presented herein uncovers very much richer physics than can be deduced from the flooding correlation in equation (1). For very long tubes (z/D=∞) no hysteresis is possible for any Prandtl number or subcooling number, and for high subcooling numbers hysteresis is possible with finite tube lengths and low Prandtl numbers. No experimental evidence exists to justify the foregoing conclusions at high subcooling numbers. At low subcooling numbers the hysteresis effect can be explained by the liquid droplets entrainment as it has been discussed above.

The generally poorer quantitative agreement in heat transfer results with the experimental data can be attributed to the poor representation of the local heat transfer process in the analysis. The heat transfer correlation for the average Nusselt number in equation (9) represents the average for the liquid subcoolings from S_{li}=.07 to S_{li}=.14 and for J_{li}^*=.05 to J_{li}^*=.16. This average is reflected in the local Nusselt number equation (21a) and, therefore, also in the analytic results presented above. Equation (9) is accurate within ±70% whereas the analytic results in Figures 10 and 11 reproduce the experimental data within ±30%. Since the experimental data for the small tube diameter in Figure 12 were not utilized in producing the correlation equation (9), the difference between the experiment and theory in this figure is 40%. The data at very low liquid volumetric fluxes in Figure 12 show considerable deviation from the theoretical prediction which is not the case for larger tube diameters in figures 10 and 11. In adiabatic flow (figures 5 and 6), the experimental data for low D^* and for low J_l^* are in good agreement with the theory. That such is not the case for the heat transfer data, can be attributed to the design peculiarities of the experiment, the methods utilized to introduce water and steam into the tube, etc.. The heat transfer flooding results in Figures 10 to 13 should be viewed as the average representation of all steam-water data for which the correlation equation (9) is valid.

The average Nusselt number in equation (9) was deduced from the low subcooling number approximation equation (6') and the experimentally measured liquid bulk temperatures. For subcooling numbers greater than .1 such a representation is not adequate for long tubes, since the average Nusselt number can be considerably underpredicted as can be seen from Figure 2. Slight inaccuracy in the power representation of z/D in equation (9) will also significantly change the numerical value of the bracket on the right of equation (21a) due to its large power dependance.

Future experimental work should attempt a more detailed study of the local heat transfer process of flooding in a tube. The analysis presented above is capable of incorporating any new developments of the local structure of the heat transfer process. The experimental data in Figures 10 to 12 were obtained by injecting water into the tube through a porous injector. Other methods of water injection might produce different results and need to be investigated. It would also be of value to extend the range of experimental data to higher subcoolings, wider range of liquid Prandtl numbers and to higher system pressures.

IV. SUMMARY AND CONCLUSIONS

An analysis has been developed to study flooding hydrodynamics and heat transfer in a tube. The hydrodynamic analysis considered local balance of gravity and viscous forces, and incorporated the effect of the liquid film-vapor core interface momentum transfer. The effect of liquid droplets entrained in the flow was taken into consideration through a simple model of the entrainment parameter.

The adiabatic flooding solution is found to depend on four parameters. These are the Bond number, D^*; ratio of gravity to viscous forces parameter, N_l; buoyancy number or density ratio parameter, Bo; and the entrainment parameter, e. Comparison of the theory with the experimental data of air-water and air-oil showed that best results are achieved for smooth tube ends with an entrainment parameter between .05 and .1. For sharp tube ends, good comparison is achieved at higher values of the liquid film volumetric flux. The effect of arbitrary parameters on flooding is illustrated by the adiabatic flooding curves in Figure 7. This parametric trend was found to be in agreement with physical observations.

In the presence of heat transfer, additional parameters are found to describe flooding in a tube. These are the subcooling number, S_{li}; liquid Prandtl number, Pr_l; and the tube length parameter, z/D. Condensation heat transfer introduces stability into the flooding curve in the sense that it raises its flooding volumetric fluxes. This stability is more pronounced for higher subcooling numbers, for lower Prandtl numbers and for lower z/D. The theory showed good qualitative and, on the average, good quantitative comparison with the experimental data of steam and water.

For steam-water flooding in a tube, the theory presented in this paper can be utilized, at the present,

as follows:

1. For low subcooling numbers, $S_{1i}<.1$, the adiabatic flooding solution of Figure 7 applies with a non-zero value of the entrainment parameter.
2. For higher subcooling numbers, $S_{1i}\geq.1$, it is conservative to utilize the adiabatic flooding solution with an entrainment parameter equal to zero. Equations (24) and (25) are very simple to use in this case.

Extrapolation of the theoretical results to high subcooling numbers revealed a hysteresis effect. This effect is more pronounced at higher subcooling numbers, at lower Prandtl numbers and for shorter tubes.

V. ACKNOWLEDGMENT

The author would like to thank Dr. J.S.K. Liu at Battelle Columbus Laboratories for supplying the steam-water flooding data.

VI. REFERENCES

1. Liu, J.S.K., Collier, R.P., and Cudnik, R.A., "Flooding of Counter-Current Steam-Water Flow In an Annulus," in "Topics in Two-Phase Heat Transfer and Flow," ASME, New York (1978).
2. Segev, A., and Collier, R.P., "Condensation and Vaporization Effects on Counter-Current Steam-Water Flow in an Annulus," in "Nonequilibrium Interfacial Transport Processes," ASME, New York (1979).
3. Liu, J.S.K., and Collier, R.P., "Heat Transfer in Vertical Counter-Current Steam-Water Flooding Flows," in "Basic Mechanisms in Two-Phase Flow and Heat Transfer," ASME, New York (1980).
4. Wallis, G.B., "One-Dimensional Two-Phase Flow," McGraw Hill, New York (1969).
5. Tien, C.L., "A Simple Analytical Model for Counter-Current Flow Limiting Phenomena With Vapor Condensation," Letters in Heat Mass Transfer, 4, pp. 231-238 (1977).
6. Tien, C.L., Chung, K.S., and Liu, C.P., "Flooding in Two-Phase Counter-Current Flows," EPRI NP-1283 (1979).
7. Bharathan, D., Wallis, G.B., and Richter, H.J., "Air-Water Counter-Current Annular Flow," EPRI NP-1165 (1979).
8. Dobran, F., "On the Consistency Conditions of Averaging Operators in Two-Phase Flow Models and On the Formulation of Magnetohydrodynamic Two-Phase Flow," Accepted for publ. Int. J. Eng. Science.
9. Lee, L., Bankoff, S.G., Yuen, M.C., Jensen, R., and Taukin, R.S., "Local Condensation Rates in Horizontal Co-Current Steam-Water Flow," in "Nonequilibrium Interfacial Transport Processes," ASME, New York (1979).
10. Wallis, G.B., "Annular Two-Phase Flow," J.Basic Eng., Trans ASME, pp. 59-82 (1970).
11. Linehan, J.H., Petrick, M., and El-Wakil, N.M., "On the Interface Shear-Stress in Annular Flow Condensation," J. Heat Transfer, Trans ASME, p. 450 (1967).
12. Kays, W.M., and Crawford, M.G., "Convective Heat and Mass Transfer," 2nd. ed. McGraw Hill, New York (1980).
13. Butterworth, D., and Hewitt, G.F., "Two-Phase Flow and Heat Transfer," Oxford Univ. Press (1977).
14. Liu, J.S.K., "Flooding Data for Counter-Current Steam-Water Flows in Tubes," Personal Communication (1980).